

One-pot synthesis of ZnFe₂O₄/C hollow spheres as superior anode materials for Lithium ion batteries

Yuanfu Deng^{ab}, Qiumei Zhang,^{bd} Shidi Tang,^a Leiting Zhang^{bc}, Shengnan Deng^{bd}, Zhicong Shi^{bd}, Guohua Chen^{bc}

^a Department of Chemistry, School of Chemistry and Chemical Engineering, South China University of Technology, Guangzhou, 510640, China;

^b Center for Green Products and Processing Technologies, Guangzhou HKUST Fok Ying Tung Research Institute, Guangzhou 511458, China; E-mail: kechengh@ust.hk

^c Department of Chemical and Biomolecular Engineering, The Hong Kong University of Science and Technology, Hong Kong, China

^d State Key Laboratory of Fine Chemicals, School of Chemical Engineering, Dalian University of Technology, Dalian 116023, China

Experimental section

2.1. Synthesis

ZnFe₂O₄/C composite materials were prepared by a low temperature solvothermal method according to the literatures with some modifications.¹ All of the reactants and solvents were analytical grade and were used without any further purification. In a typical procedure, 10 mmol of FeCl₃·6H₂O and 5 mmol of ZnCl₂ were dissolved into 35 mL of ethylene glycol (EG), adding 2 mL of PEG-600 drop to drop. Then 90 mmol of urea was added slowly under continues stirring, and a homogenous suspension was obtained. The reaction mixture was vigorously stirred for 1 h and then transferred into a Teflon-lined stainless-steel autoclave with a capacity of 50 mL for solvothermal treatment at 200 °C for 48 h. After the autoclave had cooled down to room temperature naturally, the product was centrifuged, washed with distilled water and anhydrous ethanol several times, and finally dried under vacuum at 80 °C for 12 h. The presence of EG had at least two important roles for the preparation of ZnFe₂O₄/C composite. It served not only as the solvent but also as a carbon precursor. The reacting temperature and time were both crucial to obtain the ZnFe₂O₄/C composite with hollow sphere structure. When the temperature was below 200 °C , an unkown crystal phase was obtained (Fig. S1). The strong peak at around 10° might be attributed to the formation of metal glycoalates or alkoxides derivatives by alcholysis and coordiantion of EG with the

metal ions.^{2,3} A further annealing of these intermediates at high temperature prompted their conversion into the ZnFe₂O₄/C nanoparticles (as shown in Figure S2 and S3 and EA). These particles had a tendency to aggregate. At the same time, the viscosity of EG could interfacially stabilize and reinforce the CO₂ microbubbles arising from the thermal decomposition of urea at elevated temperature, which acted as an *in situ* soft template for the aggregation of ZnFe₂O₄/C nanoparticles. Driven by the minimization force of the interfacial energy, small ZnFe₂O₄/C particles might aggregate around the gas-liquid interface and finally ZnFe₂O₄/C spheres with small hollow interior were formed via self-assemble. This is illustrated by the SEM images of the products obtained from the reaction that was kept for 12 hour at 200 °C. These spherical ZnFe₂O₄/C particles, which were congregated via nano-sized particles, present an average diameter less than 300 nm and roughened surface (Fig. S2 and S3). After that, the crystallites located in the cores, compared to those in the outer surfaces, have high surface energies and thus are easily dissolved.⁴ The nanoparticles located on the outside would serve as nucleation seeds for the subsequent crystallization process of the cores. The polycrystalline cores provided a ZnFe₂O₄/C source for the durative growth of the nanoparticles outside, and the net result of the following events should be the nanoparticles growing at the expense of the cores inside the spheres. As a result of this process, the size of the polycrystalline core was reduced gradually while the hollow volume was enlarged. Finally, the hollow sphere were formed with complete depletion of the cores, and the inner space of the spheres was further increased with a longer reacting time (48 h). Meanwhile, the diameters of the nanoparticles outside were growing bigger. All of these results could be explained by the well-known “Ostwald ripening process”,⁵ in which the initial formation of tiny crystalline nuclei in a supersaturated medium is followed by crystal growth and the larger particles grow at the cost of the small ones because of the energy difference between them.

2.2. Characterization

X-ray diffraction (XRD) patterns of the samples were obtained using a Rigaku D/Max-IIIA powder diffractmeter using Cu K α radiation at 40 kV and 40 mA at a step of 0.020. Data were recorded ranging from 10° to 80°. An energy-dispersive X-ray spectrometer (EDX) was done using a Shimadzu-EPMA1600 instrument at an accelerating voltage of 15kV. TGA was tested on TGA Q 50 instrument. Elemental analyses were performed using Perkin Elmer Optima 3000XL elemental analyzers. Field emission scanning electron microscopy (SEM) was performed on a JEOL 6300F scanning electron microscope. Transmission electron microscopy (TEM) and high-resolution transmission electron microscopy (HRTEM) were done using JEOL 2010F instruments at an accelerating voltage of 200 kV.

2.3. Electrochemical measurement

Electrochemical studies were carried out at room temperature using two-electrode cells with lithium foil as the reference and counter electrodes. The working electrodes consisted of 70% ZnFe₂O₄, 20% acetylene black and 10% polyvinylidene fluoride (PVDF) by weight and were prepared by coating the mixture on copper foils. The testing 2025 coin cells use lithium foil as counter electrode, polypropylene micro porous membrane as separator and 1M LiPF₆ dissolved in ethylene carbonate (EC), dimethyl carbonate (DMC) and ethylene methyl carbonate (EMC) (1:1:1, v/v/v) as the electrolyte. The cells were assembled in an argon-filled glove box. The cyclic Volta metric measurements were performed on a NEWARE-CT3008w Electrochemical Workstation at a scan rate of 0.1 mVs⁻¹ in a range of 3.0–0.01V vs. Li/Li⁺. The charge–discharge measurements were carried out using a BTS-55 Neware Battery charger at different current in a range of 3.0–0.01V vs. Li/Li⁺.

References

1. W. Q. Jiang, Z. Cao, R. Cu, X. Z. Ye, C. F. Jiang and X. L. Gong, *Smart Mater. Struct.*, 2009, **18**, 125013.

2. T. C. Qiu, S. H. Yang, H. Deng, L. M. Jin and W. S. Li, *J. Mater. Chem.*, 2010, **20**, 4439.
3. (a) Y. L. Wang, X. C. Jiang and Y. N. Xia, *J. Am. Chem. Soc.*, 2003, **125**, 16176; (b) X. C. Jiang, Y. L. Wang, T. herricks and Y. N. Xia, *J. Mater. Chem.*, 2004, **14**, 695; (c) A. M. Cao, J. D. Monnell, C. Matranga, J. M. Wu, L. L. Cao and D. Gao, *J. Phys. Chem. C*, 2007, **111**, 18624.
4. Z. C. Wu, K. Yu, S. D. Zhang, Y. Xie, *J. Phys. Chem. C*, 2008, **112**, 11307.
5. W. Z. Ostwald, *Phys. Chem.* 1900, **34**, 495.

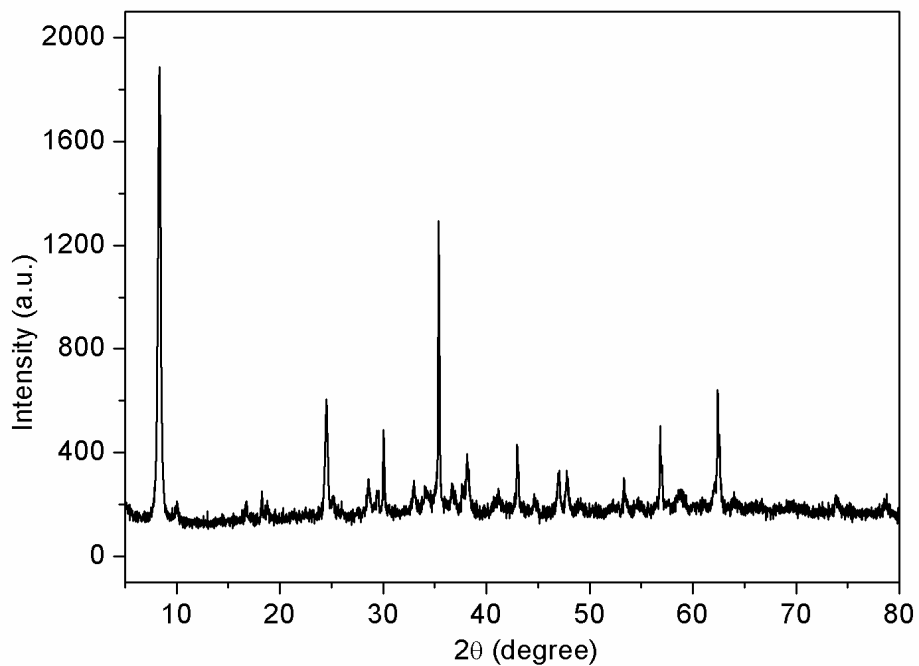


Fig. S1. The XRD pattern of the product obtained from the reaction at 180 °C for two days.

Fig. S2

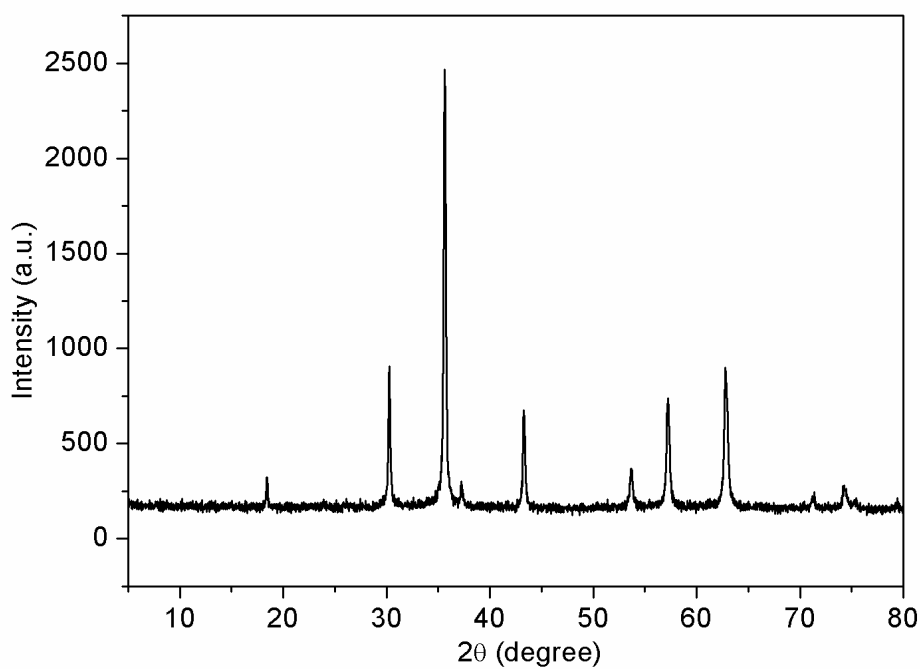


Fig. S2. The XRD pattern of the product obtained from the reaction at 200 °C for 12 hours.

Fig. S3

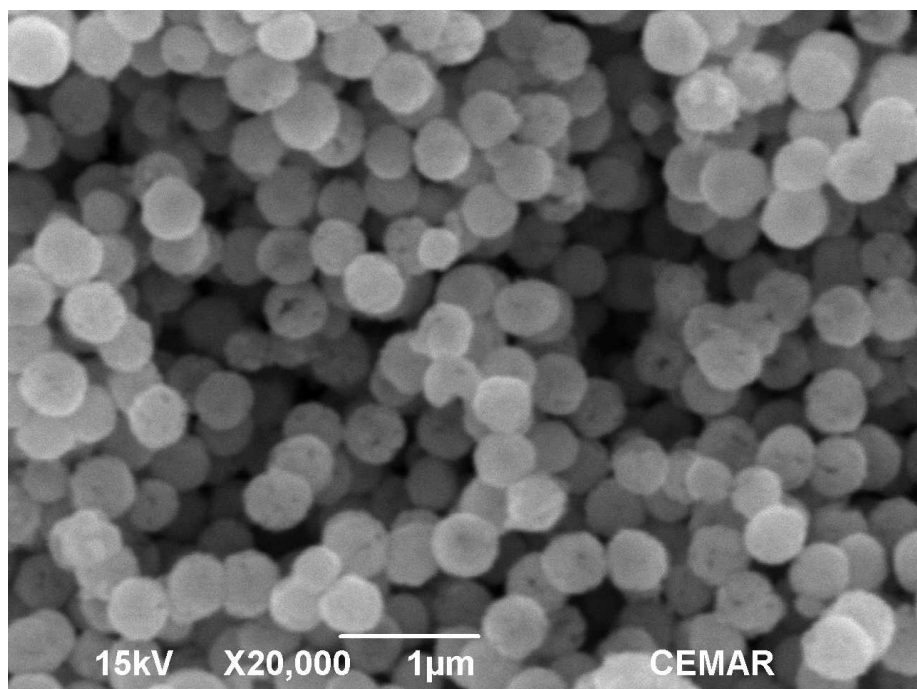


Fig. S3. The SEM image of the product obtained from the reaction at 200 °C for 12 hours.

Fig. S4

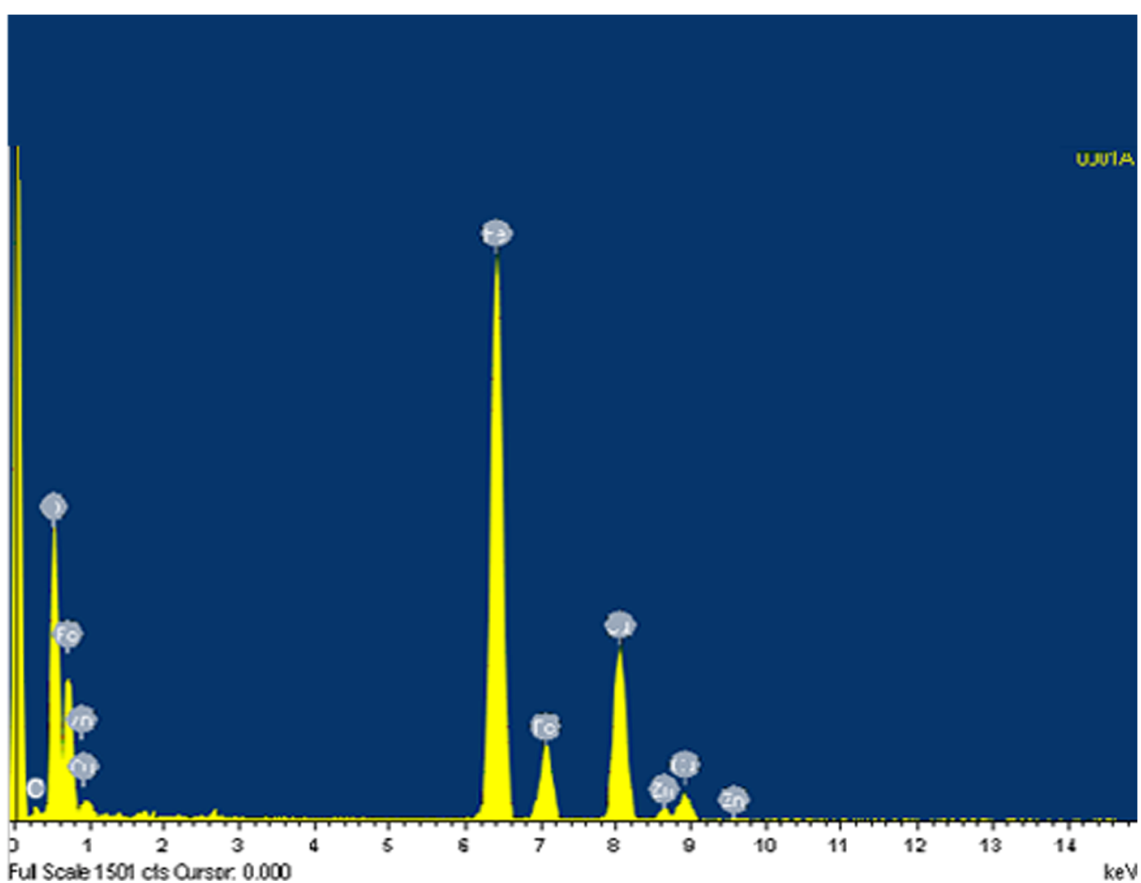


Fig. S4. The EDS of the $\text{ZnFe}_2\text{O}_4/\text{C}$ hollow spheres.

Fig. S5

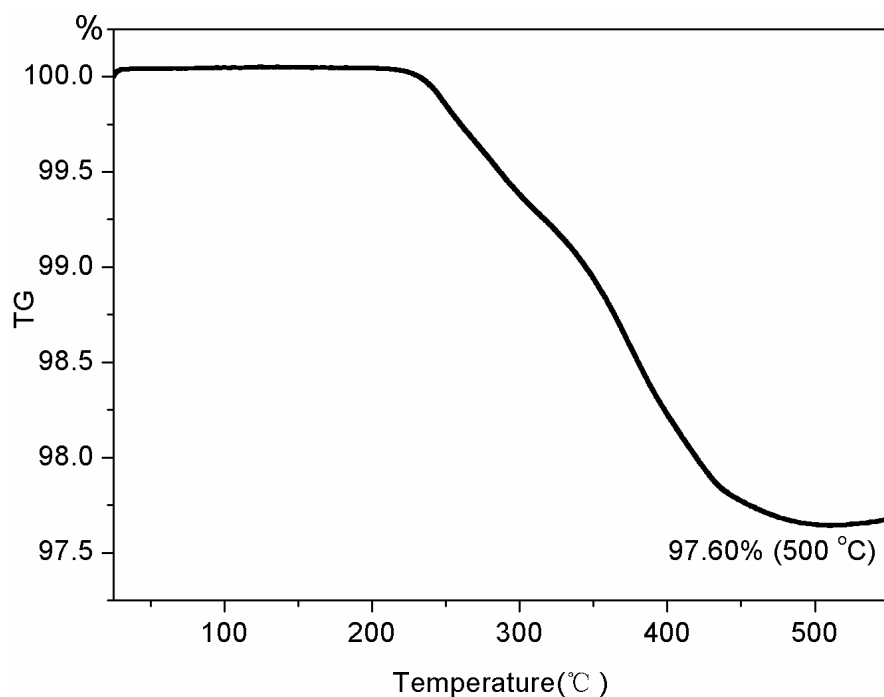


Fig. S5. The TG curve of the ZnFe₂O₄/C hollow spheres from room temperature to 550 °C.

Fig. S6

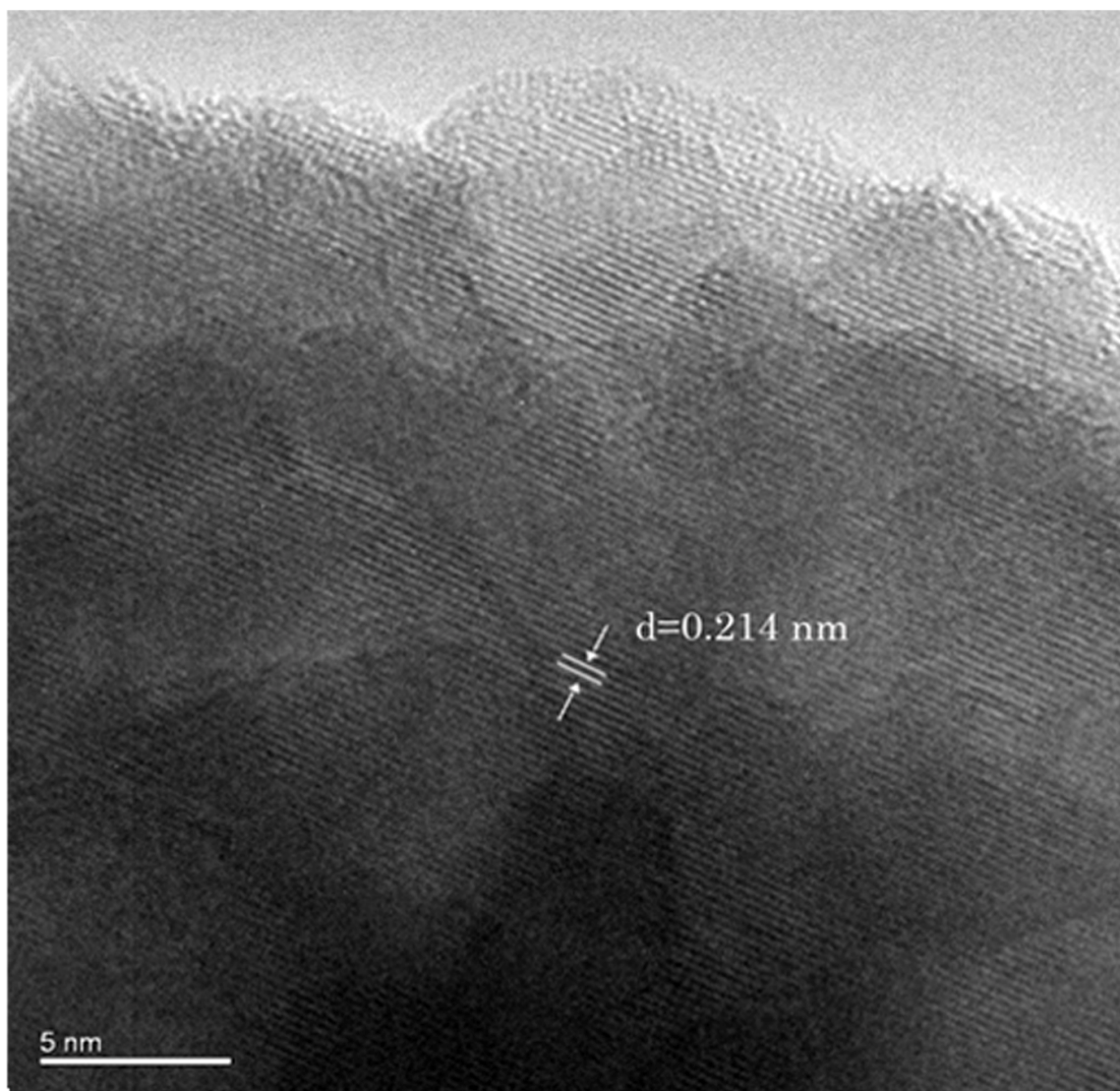


Fig. S6. The HTEM images of the ZnFe₂O₄/C hollow spheres.

Fig. S7

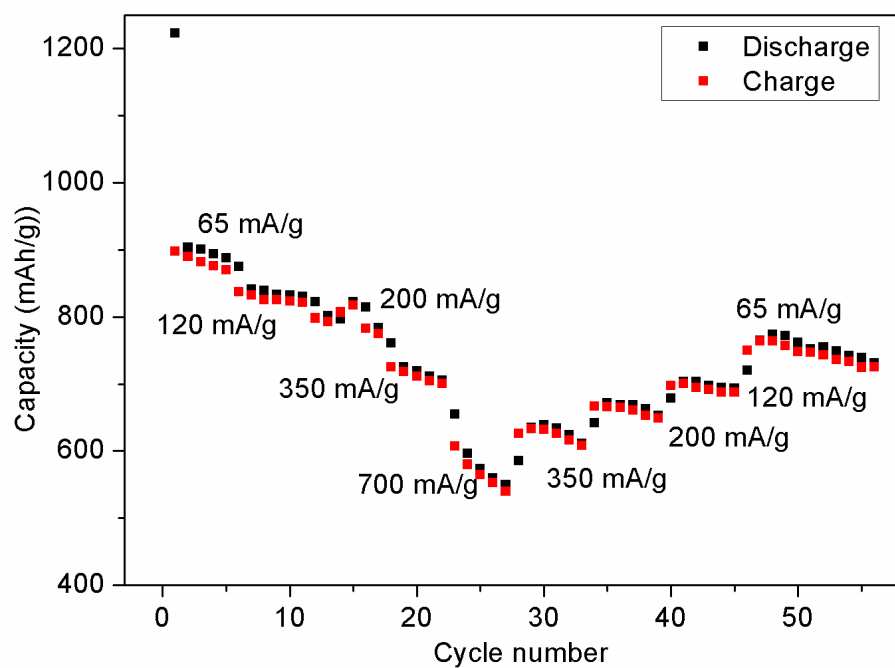


Fig. S7. The specific capacities of $\text{ZnFe}_2\text{O}_4/\text{Li}$ cell cycled at different current densities.

Fig. S8

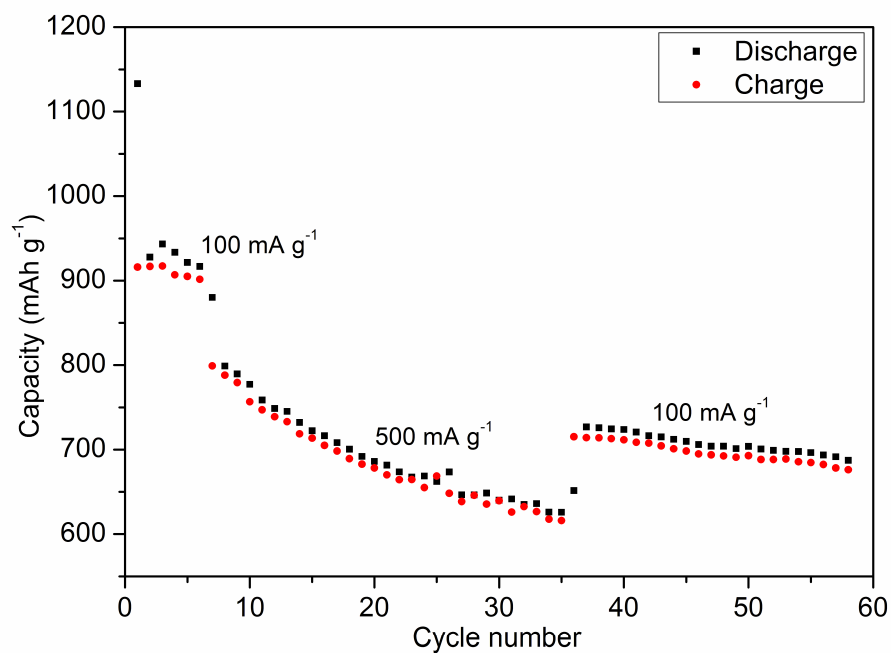


Fig. S8. The specific capacities of $\text{ZnFe}_2\text{O}_4/\text{Li}$ cell cycled at different current densities (100 mA g^{-1} for 5 cycles, 500 mA g^{-1} for 30 cycles and 100 mA g^{-1} for 20 cycles again).

Fig. S9

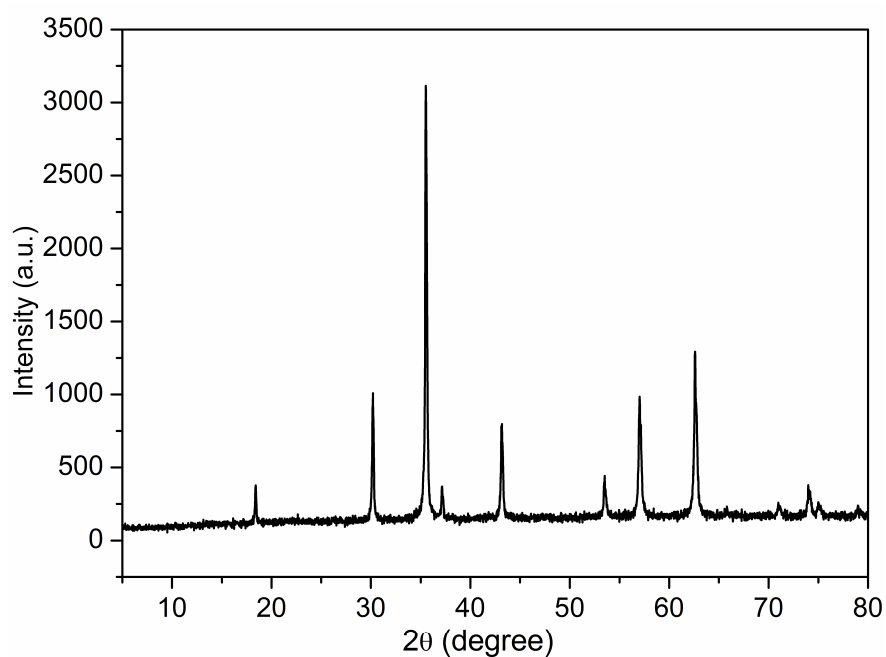


Fig. S10. The XRD pattern of the product obtained from the reaction at 200 °C for 48 hours without PEG-600.

Fig. S10

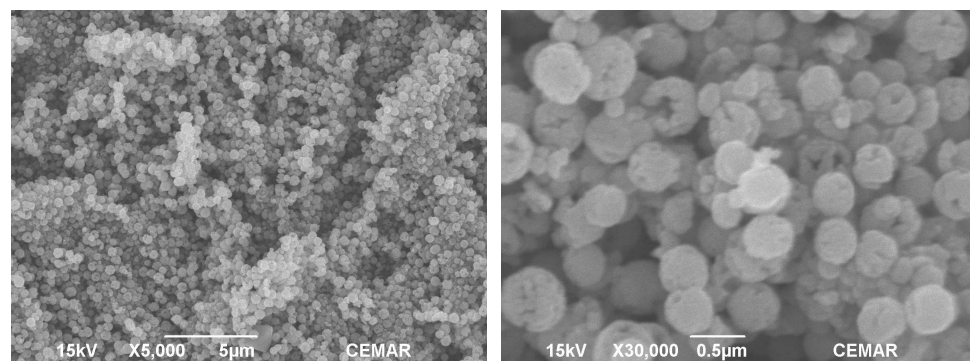


Fig. S10. The SEM image of the product obtained from the reaction at 200 °C for 48 hours without PEG-600.

Fig. S11

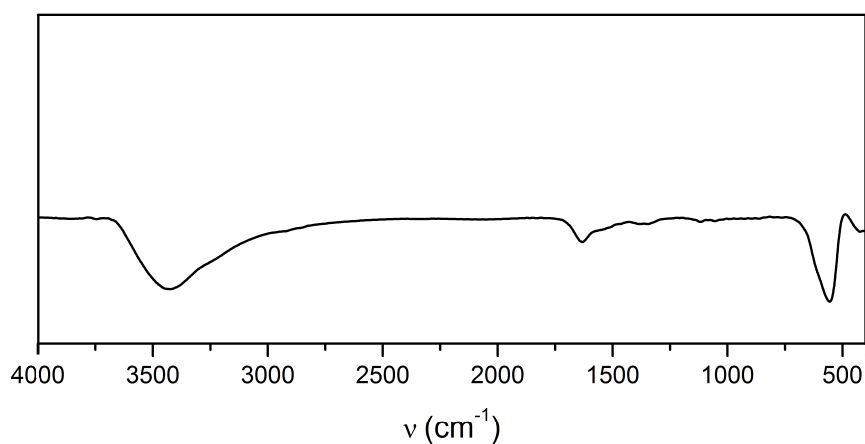


Fig. S11. The IR spectrum of the product obtained from the reaction at 200 °C for 48 hours.